Raman Spectroscopy Analysis for Precise Channel Temperature Estimation in AlGaN/GaN HEMT Devices

Marsha M. Parmar*, Robert Laishram, Preeti Garg & D.S. Rawal

Solid State Physical Laboratory, Lucknow Road, Delhi 110054, India.

Volume 1, Issue 2, March 2024
Received:11 March, 2024; Accepted: 26 March, 2024
DOI: https://doi.org/10.63015/10s-2421.1.2

**Corresponding author email: sarikamarsha@gmail.com*

Abstract: In recent years, high-electron-mobility GaN HEMTs have demonstrated significant advancements in applications such as power converters and RF amplifiers. Nevertheless, their thermal reliability poses a notable challenge, placing constraints on their power-handling capacities. This study employs micro-Raman spectroscopy to evaluate the localized self-heating-induced channel temperature. The channel temperature, determined using the single phonon modes of GaN HEMT (E2(H) & A1(LO)), exhibits discrepancies and does not align with device temperature values calculated using the SiC phonon peak near the GaN channel. However, by employing both phonon modes of GaN to decouple the combined effects of joule heating and the thermoelastic effect, accurate channel temperature values are obtained, matching well with those obtained from the SiC phonon peak. The agreement between calculated temperatures from phonon modes and those obtained by heating the device from the back side enhances the credibility of the proposed method.

Keywords: GaN HEMT, micro-Raman Spectroscopy, channel temperature, self-heating

1. Introduction: N Gallium Nitride (GaN) High Electron Mobility Transistors (HEMTs) have become pivotal components in high-frequency and high-power applications [1], [2], [3]. In GaN-based devices, the choice of substrate material, particularly between GaN-on-Si and GaN-on-SiC, introduces critical considerations for power density and thermal management [4]. The inherent limitations of GaN-on-Si, specifically associated with self-heating in the channel, impose constraints on output power density compared to GaN-on-SiC. This discrepancy is accentuated by the relatively lower thermal conductivity of single-crystalline GaN (k_{GaN} ~ 130 $Wm^{-1}K^{-1}$), comparable to silicon (k_{Si} ~ 148 $Wm^{-1}K^{-1}$), but significantly inferior to silicon carbide (k_{SiC} ~ 350 $Wm^{-1}K^{-1}$). While GaN-on-SiC, with its elevated thermal conductivity, partially alleviates thermal concerns, it falls short of fully unleashing the potential of GaN HEMTs in terms of both direct current (DC) and radio frequency (RF) powers due to suboptimal heat dissipation. Recent advancements, exemplified by GaN-on-diamond substrates boasting superior thermal conductivity ($k_{diamond}$ ~ 1800 $Wm^{-1}K^{-1}$), present a promising avenue for mitigating the thermal limitations of GaN HEMTs. GaN-on-diamond configurations have demonstrated record-breaking DC power densities of up to 56 Wmm-1, surpassing traditional substrates [5]. The heightened power density directly translates into a more expansive safe operating area (SOA) for power transistors. This introduction lays the groundwork for our research, which focuses on the integration of diamond as a chip-level heat spreader for GaN HEMTs.

Before exploring various thermal management strategies, accurately determining the channel temperature is crucial. Raman spectroscopy, with a spatial resolution of 1-2µm, has been extensively researched for determining localized self-heating-induced device temperature as an alternative to IR thermography, which has a spatial resolution of 5µm [6]. Raman spectroscopy, a non-

destructive technique, enables the estimation of channel temperature with a resolution better than 2µm. This method relies on the interaction of light with materials at the molecular level. Its widespread use in studying the properties of group III nitrides is attributed to their strong Raman activity. In the Raman scattering process, a photon of wavelength λ_0 from the excitation source, typically a narrow linewidth laser, undergoes inelastic scattering to a different wavelength λ by emitting (Stokes process) or absorbing (anti-Stokes process) an optical phonon in the sample. Each allowed optical phonon mode appears as a peak with a centroid ω and linewidth Γ, related to the phonon frequency and lifetime. The Raman peak position $\omega = \lambda_0^{-1} - \lambda^{-1}$, specified in units of cm^{-1}, is proportional to the phonon frequency, and the linewidth Γ reflects the phonon lifetime. Given that phonon frequencies, lifetimes, and populations vary with temperature, micro-Raman spectroscopy in GaN HEMTs employs Stokes peak positions, Stokes peak linewidths, and/or Stokes/anti-Stokes intensity ratios for temperature measurement [7]. It is noteworthy that although Raman Spectroscopy provides better resolution than IR, the former takes longer time to collect the data. The relationship between Raman peak shifts and temperature/stress is not uniquely defined and can vary depending on factors such as material composition, sample geometry, and measurement conditions.

In the subsequent section, we delve into the details of in-situ Raman measurements conducted on in-house fabricated GaN HEMTs to determine channel temperature during external bias application, addressing self-heating effects. For this purpose, we devised an integrated electrical setup capable of delivering DC bias to the GaN HEMTs while concurrently conducting temperature measurements. In our study, we utilized two key GaN phonon modes: E2(H) and A1(LO). These phonon modes exhibit combined responses to temperature variations and stress-induced shifts in peak positions. To separate the temperature and stress contributions, we utilized mathematical models that incorporate both temperature and stress terms into the analysis of Raman peak shifts. By simultaneously analyzing the changes in peak positions and linewidths of both E2(H) and A1(LO) phonon modes, we were able to establish relationships between temperature, stress, and Raman peak shifts. This approach allowed us to quantitatively determine the temperature and stress components contributing to the observed Raman peak shifts, thereby enabling a more accurate estimation of the channel temperature in GaN HEMT devices.

2. Experimental Details: For the in-situ measurement of the channel temperature during the application of a DC bias, we designed and fabricated a printed circuit board (PCB) using the toner transfer method. To enhance the PCB's suitability for wire bonding, we applied a 3µm thick gold electroplating process to cover the entire board. Subsequently, banana jack connectors were soldered to the PCB to ensure a robust connection. Special attention was given to ensuring that the PCB precisely matched the dimensions of the substrate holder hole in the Raman setup, minimizing any potential movement during in-situ measurements. The devices were bonded to the PCB using a TPT

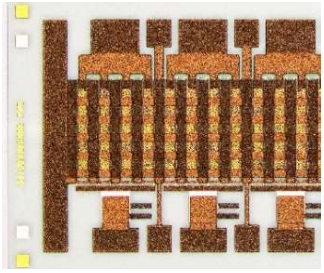

wire bonder. GaN HEMTs, grown through

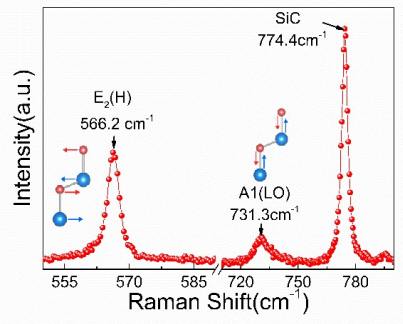

metal-organic chemical vapor deposition on a

Figure1(a) Optical micrograph of final device after fabrication. $L_g = 0.4\mu m$, $L_{sd} = 4\mu m$, $L_{gg} = 60\mu m$, Unit gate width = 300-400μm. (b) Raman Spectroscopy of GaN HEMT under ambient condition.

SiC substrate, were investigated. These devices featured a 25nm AlGaN layer on top of HEMT with increasing V_{ds} due to self-heating. The phonon peak positions of GaN, namely E2(H) and A1(LO), as well as that of SiC, shift2µm doped GaN buffer layer. Standard Ti/Al/Ni/Au Ohmic contacts and Ni/Au Schottky gates were employed in the design, with a source-drain separation of 4µm, a gate length of 0.4µm, and a gate-to-gate distance of 60µm in a multifinger configuration, as illustrated in the optical micrograph in Figure 1a. The operation involved applying a DC source-drain bias ranging from 0 to 6 V and a -2.7 V gate voltage. Micro-Raman measurements were conducted using a Horiba spectrometer with a 532 nm frequency-doubled Nd:YAG laser as the excitation source. The sub-bandgap laser illumination was carefully chosen to ensure minimal laser absorption, avoiding interference with device operation during measurements. The experimental setup adopted ZX,−Z Raman backscattering configuration with unpolarized detection, allowing simultaneous measurement of the A1(LO) (out-of-plane) and E2(H) (in-plane) phonon modes of GaN. Figure 1b depicts a Raman spectrum obtained from an in-house fabricated GaN HEMT under unbiased conditions, revealing the presence of the two most common modes of GaN, namely E2(H) (in-plane, 568.5 cm^{-1}) and A1(LO) (out-of-plane, 736.5 cm^{-1}). The reported wavenumbers correspond to the unstrained GaN layer. However, in the context of HEMT devices where GaN is grown on different materials, such as SiC, mismatches in lattice constants and thermal expansion coefficients occur. Consequently, even under unbiased conditions, shifts from the nominal peak frequencies were observed, as illustrated in Figure 1b. A red shift in the mentioned phonon peak positions signifies an overall tensile strain in the device, while a blue shift indicates compressive strain. We used 532 nm laser light for recording Raman spectra, allowing only 25% of the laser power to fall on the sample to avoid heating. A 50X LWD objective was usedfor focusing, and the spot size was approximately 2.5µm. The Raman spectra were recorded at a spot between the drain and source, as shown in the inset of Figure 2a. The spectra were recorded at a gate bias of -2.7V while the source-to-drain voltage was swept from 0V to 6V. To prevent overheating, since no active cooling was applied, the current compliance was kept at 500mA. The Raman spectroscopy data provides an examination of average temperatures across the 2 µm thickness of the GaN stack layer in our devices. The depth of focus (DOF) extends beyond the thickness of the GaN layer, enabling the collection of signals from SiC phonon modes in close proximity to the GaN layer. Figure 2a

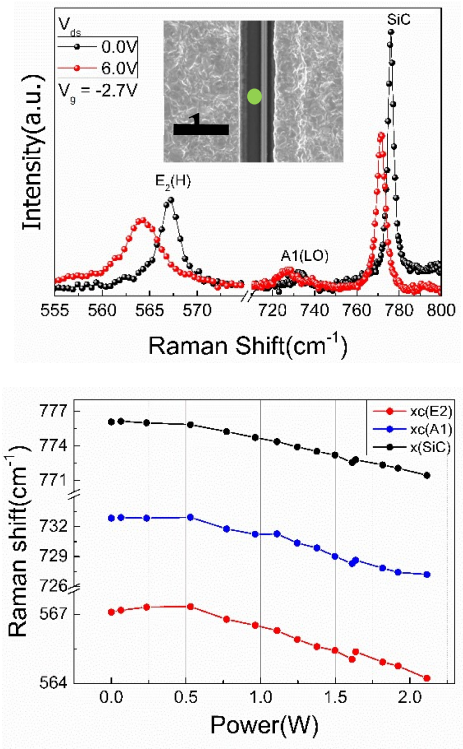

Figure 2(a) Raman Spectra of GaN HEMT. The black curve shows the Raman peaks at 0 V bias condition while the pink one shows the Raman spectra at V_{ds} = 6.0V. The curves show a clear shift in Raman peaks due to self-heating under biased condition. (b)The observed shift in Raman peaks of optical phonon modes for E_2(H), A_1(LO) and SiC under biased condition due to self-heating.

clearly shows a shift in both in-plane (E2(H)) and out-of-plane (A1(LO)) modes of GaN

towards the lower wavenumber side. Figure 2b illustrates the Raman shift in GaN and SiC spectra as a function of applied power to the device.

3. Results and Discussion: The generation of the Raman scattering spectrum is intricately linked to the lattice vibrations of the sample. When subjected to tensile or compressive residual stress, the atomic bond lengths adjust, altering the lattice vibration energy. The frequency shift in the Raman spectrum is sensitive to the sample's temperature and stress. $\omega(T) = \omega_0 + \frac{A}{e^{Bhc/kT}-1}$ (1)

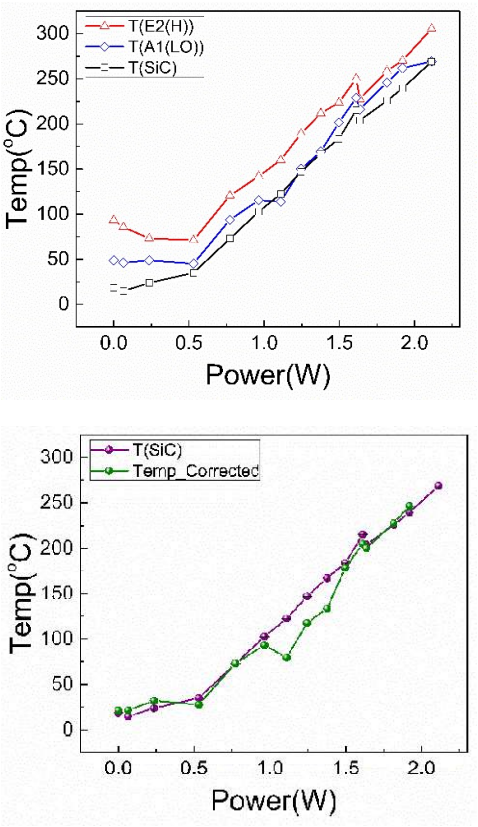

Figure 3(a) Calculated channel temperature versus biased power of GaN HEMT assuming the shift in phonon frequencies is only due to heating (eq 1). (b) Calculated in channel temperature taking into account the shift in the phonon frequencies as a combined effect of heating and thermal stress (eq 2).

where, $\omega(T)$ is the Raman peak position at temperature T in kelvin, ω_0 is the Raman peak position at absolute zero, A and B are empirical constants determined by calibration [7]. Using above equation one can calculate the temperature of the device form just one phonon peak. The estimated temperature from all the three peaks namely E2(H), A1(LO) and SiC are shown in Figure a. It must be noted that the temperature calculated from each of the peak using equation has a difference of $\sim 50℃$ moreover, the base temperature as calculated by E2(H) peak suggests that the device temperature at 0 bias is $\sim 100℃$ which is 75℃ more than the room temperature. This means the shift in the peaks due to self-heating is not entirely the effect of increase in local temperature but has contribution from another factor. It turns out that stress also affects phonon frequencies and can therefore also be determined using Raman spectroscopy. However, the key challenge is that phonon frequency changes induced by thermal stress are superimposed on the direct temperature induced change, and are typically much smaller. By combining information from both phonon modes, namely E2(H) and A1(LO) we can simultaneously determine temperature and thermal stress from the Raman measurement. Eq (1) can be modified to include thermal stress as [9],

$$\omega(T) = \omega_0 + \frac{A}{e^{Bhc/kT}-1} - 2a'\varepsilon_{xx} \quad (2)$$

where, a' is empirical constant and ε_{xx} is biaxial strain. If we use equation 2 and calculate the temperature excluding the contribution of stress, it matches well with SiC temperature as shown in Figure (b). The SiC does not have a lattice mismatch during growth so it does not have the effect of thermal stress, hence for SiC, one phonon peak is enough for temperature estimation. Both the E2(H) and A1(LO) phonon modes exhibit responses to temperature variations and thermoelastic effects in the form of shifts in above phonon peak positions. For decoupling the effect of joule heating with that of thermoelastic effects in phonon peaks we used equation 2. Now to calculate the values of these two variables, we formed two equations using the shift in the peak position of E2(H) and A1(LO) phonon modes which change with increase in bias voltage. These two equations when simultaneously solved together, decouple the

combined effect of joule heating and thermoelastic effect. By analyzing the changes in peak positions of both phonon modes simultaneously, we were able to differentiate between the contributions of temperature and stress to the observed shifts in Raman peaks.

Moreover, the unbiased temperature values also drop to also drops to 22℃ which was the ambient temperature. The discrepancies between temperatures obtained using single phonon modes of GaN and the SiC peak primarily arise due to the difference in lattice mismatch during the growth of GaN on SiC. The lattice mismatch between SiC and GaN is 3.5% which gives rise to thermoelastic stress under dc biased condition. So the shift in phonon modes of GaN (namely E2(H) & A1(LO)) has combined effect of joule heating and thermoelastic effect. While for SiC, there is no lattice mismatch condition. Hence the shift in the peak is entirely due to joule heating. Also, since the DOF of the Raman microscope for 532 nm laser is 2um, the temperature calculated form SiC peak is almost equal to the channel temperature. The use of equation 2 decouples the combined effect of joule heating and thermoelastic effect for GaN using two phonon modes. Whereas for SiC since the later effect is not present equation 1 is able to provide the correct result. In our study, Raman spectroscopy plays a crucial role in determining the peak operating temperature of GaN HEMT devices, which we identified to be 200°C. This temperature, corresponding to a specific bias condition (e.g., Vgs = -2.7V and Vds = 6V), represents a critical parameter for assessing device performance and thermal reliability. The determination of this peak operating temperature is facilitated by analyzing the shifts in Raman peaks, particularly those associated with the E2(H) and A1(LO) phonon modes of GaN. These shifts in peak positions, observed under biased conditions, reflect the combined effects of joule heating and thermoelasticity within the device structure. By meticulously analyzing the Raman data collected under varying bias voltages and conditions, we were able to identify the temperature at which the device operates optimally, corresponding to the peak operating temperature of 200°C. This temperature not only provides crucial insights into the thermal behavior of GaN HEMTs but also serves as a reference point for evaluating device performance and reliability under different operating conditions. Furthermore, the agreement between the peak operating temperature determined from Raman spectroscopy and the observed device temperature during backside heating experiments reinforces the credibility and accuracy of our method. This alignment underscores the effectiveness of Raman spectroscopy in providing precise temperature estimations, thereby enhancing our understanding of thermal management strategies in GaN HEMT devices.

Again, to back check the calculated channel temperature, we heated the device form back side using a thermal chuck and noted the shift in peak position and compared it with the temperature values obtained during self-heating. The results are plotted in Figure . Hence, the true channel temperature can be characterized by assuming the shift in phonon frequencies as a combined effect of heating

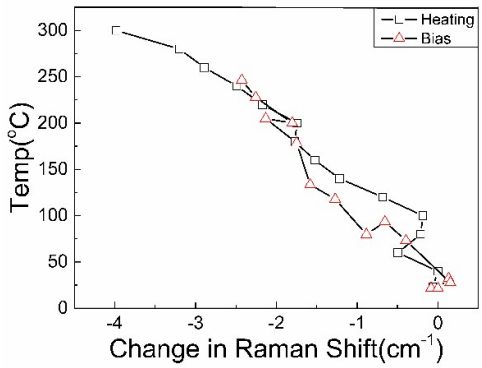

Figure 4 Comparison of the channel temperatures while heating the device from backside with that of self-heating.

and thermal stress which matches well with the channel temperature of the device while heating from back-side.

4. Conclusions: Raman spectroscopy offers insights into the vibrational characteristics of GaN and SiC, revealing sensitivity to factors

such as crystalline quality, temperature, stress, and free carrier density. By employing two phonon modes to separate temperature and stress components, it allows for a more precise determination of channel temperature. The identified peak operating temperature is 200℃ at V_{gs} = -2.7V and V_{ds} = 6V, aligning closely with the device temperature observed during backside heating. This research sheds light on the critical issue of thermal reliability in GaN HEMTs, offering detailed insights into temperature effects through micro-Raman spectroscopy. The agreement between calculated temperatures and SiC characterization enhances the credibility of the proposed method.

Acknowledgement: We gratefully acknowledge Director SSPL and GaN team at SSPL & GAETEC for fabrication and SSPL characterization division for all the support.

Conflict of Interest: Authors declare No conflicts of interest.

References:

[1]X. Yang *et al.*, "Dynamic RON Free 1.2-kV Vertical GaN JFET," *IEEE Transactions on Electron Devices*, vol. 71, no. 1, pp. 720–726.
[2]Y. Liao, H. Li, K. Qu, and X. Liu, "A Novel Inverse-L Buried GaN Current-Aperture Vertical Electron Transistors," in *2023 Cross Strait Radio Science and Wireless Technology Conference (CSRSWTC).*
[3]D. Wang, D. H. Mudiyanselage, and H. Fu, "Design of kV-Class and Low RON E-Mode β-Ga2O3 Current Aperture Vertical Transistors With Delta-Doped β-(AlxGa1−x)2O3/Ga2O3 Heterostructure," *IEEE Transactions on Electron Devices*, vol. 70, no. 11, pp. 5795–5802.
[4]J. Kuzmik *et al.*, "Self-Heating in GaN Transistors Designed for High-Power Operation," *IEEE Transactions on Electron Devices*, vol. 10, no. 61, pp. 3429–3434, 2014,
[5]M. J. Tadjer *et al.*, "GaN-On-Diamond HEMT Technology With TAVG = 176°C at PDC,max = 56 W/mm Measured by Transient Thermoreflectance Imaging," *IEEE Electron Device Letters*, vol. 40, no. 6, pp. 881–884,.
[6]"A Review of Raman Thermography for Electronic and Opto-Electronic Device Measurement With Submicron Spatial and Nanosecond Temporal Resolution | IEEE Journals & Magazine | IEEE Xplore."
[7]A. Sarua *et al.*, "Integrated micro-Raman/infrared thermography probe for monitoring of self-heating in AlGaN/GaN transistor structures," *IEEE Transactions on Electron Devices*, vol. 53, no. 10, pp. 2438–2447.
[8]M. S. Liu, L. A. Bursill, S. Prawer, K. W. Nugent, Y. Z. Tong, and G. Y. Zhang, "Temperature dependence of Raman scattering in single crystal GaN films," *Applied Physics Letters*, vol. 74, no. 21, pp. 3125–3127.
[9]T. Batten, J. W. Pomeroy, M. J. Uren, T. Martin, and M. Kuball, "Simultaneous measurement of temperature and thermal stress in AlGaN/GaN high electron mobility transistors using Raman scattering spectroscopy," *Journal of Applied Physics*, vol. 106, no. 9, p. 094509.